BIOCHEMISTRY
including biophysical chemistry & molecular biology

Article

Kinetics and Thermodynamics of Phalloidin Binding to Actin Filaments from Three Divergent Species

Enrique M. De La Cruz, and Thomas D. Pollard

More About This Article

Additional resources and features associated with this article are available within the HTML version:

- Supporting Information
- Links to the 1 articles that cite this article, as of the time of this article download
- Access to high resolution figures
- Links to articles and content related to this article
- Copyright permission to reproduce figures and/or text from this article

View the Full Text HTML

ACS Publications
High quality. High impact.

Kinetics and Thermodynamics of Phalloidin Binding to Actin Filaments from Three Divergent Species[†]

Enrique M. De La Cruz and Thomas D. Pollard*

Department of Cell Biology & Anatomy, The Johns Hopkins University School of Medicine, 725 North Wolfe Street, Baltimore, Maryland 21205

ABSTRACT: We compared the kinetics and thermodynamics of rhodamine phalloidin binding to actin purified from rabbit skeletal muscle, *Acanthamoeba castellanii*, and *Saccharomyces cerevisiae* in 50 mM KCl, 1 mM MgCl$_2$, and pH 7.0 buffer at 22 °C. Filaments of *S. cerevisiae* actin bind rhodamine phalloidin more weakly than *Acanthamoeba* and rabbit skeletal muscle actin filaments due to a more rapid dissociation rate in spite of a significantly faster association rate constant. The higher dissociation rate constant and lower binding affinity of rhodamine phalloidin for *S. cerevisiae* actin filaments provide a quantitative explanation for the inefficient staining of yeast actin filaments, compared with that of rabbit skeletal muscle actin filaments [Kron *et al.* (1992) *Proc. Natl. Acad. Sci. U.S.A. 89*, 4466−4470]. The temperature dependence of the rate constants was interpreted according to transition state theory. There is a small enthalpic difference ($\Delta H^\ddagger$) between the ground states and the transition state. Consequently, the free energy of activation ($\Delta G^\ddagger$) for association and dissociation of rhodamine phalloidin is dominated by entropic changes ($\Delta S^\ddagger$). At equilibrium, rhodamine phalloidin binding generates a positive entropy change ($\Delta S°$). The rates of rhodamine phalloidin binding are independent of the pH, ionic strength, and filament length. Rhodamine covalently bound decreases the association rate and affinity of phalloidin for actin. The association rate constant is low for both phalloidin and rhodamine phalloidin because the filaments must undergo conformational changes (*i.e.* "breathe") to expose the phalloidin binding site [De La Cruz, E. M., & Pollard, T. D. (1994) *Biochemistry 33*, 14387−14392]. Raising the solvent microviscosity, but not the macroviscosity, dampens these conformational fluctuations, and phalloidin binding kinetics are inhibited. Yeast actin filaments bind rhodamine phalloidin more rapidly, suggesting that perhaps they are more flexible and can breathe more easily than rabbit or *Acanthamoeba* actin filaments.

Phalloidin, a heptapeptide toxin from the poisonous mushroom *Amanita phalloides*, binds tightly and specifically to polymerized actin, stabilizing the filaments from a variety of depolymerizing agents and conditions (Wieland & Faulstich, 1978). Phalloidin decreases the critical concentration for actin polymerization by reducing the dissociation rate constant of monomers from filament ends (Estes *et al.*, 1981). An atomic model of the actin filament (Lorenz *et al.*, 1993) places phalloidin at the interface of three actin subunits, where it could stabilize subunit interactions.

The association rate constant for rhodamine phalloidin binding to actin filaments ($\sim$3 × 10^4 M^{-1} s^{-1}) is much slower than the association rate constants of other actin binding proteins (De La Cruz & Pollard, 1994; Allen & Janmey, 1994). For example, the association rate constants of myosin subfragment-1 (Blanchoin *et al.*, 1996), gelsolin (Allen & Janmey, 1994), filamin (Goldman & Isenberg, 1993), and α-actinin (Kuhlman *et al.*, 1994) are all $\sim$10^6−10^7 M^{-1} s^{-1}. The slow association rate constant of rhodamine phalloidin suggests that not all of the phalloidin binding sites on a filament are readily available but become accessible as the filament experiences thermal fluctuations in shape, or "breathes" (De La Cruz & Pollard, 1994).

We have compared the kinetics and thermodynamics of rhodamine phalloidin binding to actin filaments from three divergent species: New Zealand white rabbits, *Acanthamoeba castellanii*, and *Saccharomyces cerevisiae*. In each case, binding is driven by a large entropy change. A single amino acid substitution in the phalloidin binding site of the yeast actin may explain its lower affinity for rhodamine phalloidin. The effects of salt, pH, and viscosity demonstrate the importance of actin filament dynamics for phalloidin binding. In addition, we present the kinetic and equilibrium constants for phalloidin binding to rabbit muscle actin filaments.

MATERIALS AND METHODS

Reagents. Salts, buffers, ethylene glycol bis(β-aminoethyl ether)-*N,N,N′,N′*-tetraacetic acid (EGTA), NaN$_3$, protease inhibitors, glass beads, Sephadex G-150, methylcellulose, phalloidin, and grade I adenosine 5′-triphosphate (ATP) were obtained from Sigma Chemical Co. (St. Louis, MO). Dithiothreitol, formamide (purity of >99%), and DNase 1 were purchased from Boehringer Mannheim Corp. (Indianapolis, IN). DNase 1 was coupled to Affigel (Biorad, Hercules, CA) essentially as described by Cook and Rubenstein (1992). Guanidine hydrochloride and sucrose (Ultra Pure) were obtained from ICN Biomedicals, Inc. (Aurora, OH). DEAE-DE52 was from Whatman (Fairfield, NJ). D$_2$O was kindly provided by Dr. V. K. Vinson. Molecular Probes (Eugene, OR) and Sigma Chemical Co. (St. Louis, MO) sold us rhodamine phalloidin. There were no significant differ-

ences in binding kinetics between the rhodamine phalloidin from the two suppliers (data not shown). The concentrations of phalloidin stock solutions were determined by absorbance using $\epsilon_{300} = 1.07 \times 10^4$ M^{-1} cm^{-1} for phalloidin in water (Miyamoto *et al.*, 1986) and $\epsilon_{540} = 7.25 \times 10^4$ M^{-1} cm^{-1} for rhodamine phalloidin in methanol (Molecular Probes).

Actin Purification and Modification. Rabbit skeletal muscle actin was purified by the method of Spudich and Watt (1971). *A. castellanii* actin was purified according to Pollard (1984). The final step in both preparations was gel filtration on Sephadex G-150 or Sephacryl S-300 equilibrated in buffer A [0.2 mM ATP, 0.5 mM DTT, 0.1 mM CaCl$_2$, 1 mM NaN$_3$, and 2 mM Tris (pH 8.0)] at 4 °C (MacLean-Fletcher & Pollard, 1980). Skeletal muscle and *Acanthamoeba* actin concentrations were determined by absorbance at 290 nm using $\epsilon = 2.66 \times 10^4$ M^{-1} cm^{-1} (Houk & Ue, 1974).

S. cerevisiae actin was purified by the method of Cook and Rubenstein (1992). Briefly, ~80 g of a pressed yeast cake (kindly provided by Dr. Carl Frieden of Washington University School of Medicine, St. Louis) was disrupted with glass beads (425−600 μm, acid-washed) in a Dyno-Mill Model KDL bead mill (Glen Mills Inc., Clifton, NJ) at 4 °C in ~150 mL of buffer A′ (buffer A with the pH adjusted to 7.5) free of DTT and azide and supplemented with protease inhibitors (1 μg/mL aprotinin, antipain, leupeptin, pepstatin A, chymostatin, 2 μg/mL soybean bovine trypsin inhibitor, and 0.3 mM PMSF). The lysate was passed through three layers of cheese cloth to remove the glass beads and centrifuged at 128000*g* for 45 min. The supernatant was applied to a DNase 1 column equilibrated in buffer A′. Actin was eluted with 50% formamide/1X buffer A and applied directly to a 2.5 mL DEAE-DE52 column. Actin was eluted from the DEAE with 0.3 M KCl/1X buffer A. Peak fractions were pooled and dialyzed overnight against buffer A, polymerized with 2 mM MgCl$_2$ and 50 mM KCl, and then pelleted at 208000*g*. The actin pellet was dialyzed against buffer A for 2 days, and actin oligomers were removed by centrifugation. Actin was stored on ice and used within 10 days. Purified actin migrated as a single band with an apparent molecular mass of ~43000 Da as determined by SDS−PAGE. The concentration was determined by BCA protein assay (Pierce) using *Acanthamoeba* actin as a standard.

Mg^{2+}−actin was made by adding 200 μM EGTA and 80 μM MgCl$_2$ to Ca^{2+}−actin in buffer A essentially as described (Gershman *et al.*, 1989; Kinosian *et al.*, 1991). Actin was polymerized by adding 0.1 volume of 10X KMEI [500 mM KCl, 10 mM MgCl$_2$, 10 mM EGTA, and 100 mM imidazole (pH 7.0)] to Mg^{2+}−actin to generate a stock solution of actin filaments in 1X polymerizing buffer.

Determination of the Critical Concentration. The critical concentration for assembly was measured by 90° light scattering (λ_{ex} and λ_{em} = 400 nm) at 22 °C in 1X polymerizing buffer after diluting a stock polymer solution to the indicated actin concentrations, sonicating briefly in a bath sonicator, and equilibrating at 22 °C for 4 h. Under our experimental conditions *S. cerevisiae* actin has a critical concentration of 0.15 μM (data not shown). Rabbit skeletal muscle and *Acanthamoeba* actin have critical concentrations of 0.1 μM.

Rhodamine Phalloidin Binding Kinetics. The observed rate constant (k_{obs}) for rhodamine phalloidin binding to actin

filaments was determined by measuring the time course of fluorescence intensity increase (λ_{ex} = 550 nm, λ_{em} = 575 nm) after mixing equal volumes of 20−40 nM rhodamine phalloidin with varying concentrations of Mg^{2+}−F-actin each in 1X polymerizing buffer (De La Cruz & Pollard, 1994). The dissociation rate constant of the rhodamine phalloidin−actin complex (k_{-RhPh}) was determined by displacing bound rhodamine phalloidin with excess unlabeled phalloidin (De La Cruz & Pollard, 1994).

The temperature dependence of the rate constants was analyzed according to transition state theory (Eyring, 1935; Fersht, 1984) which relates the rate constant of a reaction to an equilibrium constant between the reactants and the transition state, a transient high-energy species that decays to form product. The free energy of activation ($\Delta G^{\ddagger}$) for formation of the transition state is related to the rate constant (k) of a reaction by

$$\Delta G^{\ddagger} = -RT \ln\left(\frac{kh}{k_B T}\right) \tag{1}$$

where h is Planck's constant, k_B is Boltzmann's constant, R is the gas constant, and T is the absolute temperature in Kelvin. The transmission coefficient (Eyring, 1935) is assumed to be unity (Fersht, 1984) and can be ignored. The free energy of activation can be expanded into its enthalpic ($\Delta H^{\ddagger}$) and entropic ($\Delta S^{\ddagger}$) components to yield the equation

$$\Delta H^{\ddagger} - T\Delta S^{\ddagger} = -RT \ln\left(\frac{kh}{k_B T}\right) \tag{2}$$

Rearranging, we obtain

$$\ln\left(\frac{kh}{k_B T}\right) = \left(\frac{-\Delta H^{\ddagger}}{R}\right)\left(\frac{1}{T}\right) + \frac{\Delta S^{\ddagger}}{R} \tag{3}$$

The enthalpy of activation ($\Delta H^{\ddagger}$) is obtained from the slope of the line generated by plotting the left-hand side of the equation versus the inverse absolute temperature. The intercept yields the entropy of activation ($\Delta S^{\ddagger}$), but it is not an accurate determination due to the long extrapolation beyond the range of the data. The activation entropy ($\Delta S^{\ddagger}$) at a given temperature is determined from

$$\Delta S^{\ddagger} = \frac{\Delta H^{\ddagger} - \Delta G^{\ddagger}}{T} \tag{4}$$

Isothermal Titration Calorimetry (ITC). The enthalpy change ($\Delta H°$) associated with phalloidin binding was measured directly with an Omega titration calorimeter (MicroCal, Inc.). A single aliquot of a concentrated rhodamine phalloidin solution was injected into a solution of 5 μM actin filaments so that all sites would be occupied upon equilibration. A second injection served to correct for nonspecific heats arising from mixing. Both phalloidin and actin were in 1X polymerizing buffer, and the temperature was 25 °C. Data analysis was done with software accompanying the instrument as instructed by the manufacturer (MicroCal Software, Inc.).

Solvent Manipulations. The pH was adjusted with MES for pH 5.90−6.50, imidazole for pH 6.90−7.35, or Tris for pH 7.85−8.34. The ionic strength was adjusted with KCl in the rhodamine phalloidin syringe (for k_+ determinations) or by diluting a concentrated aliquot of actin−rhodamine

phalloidin in 1X polymerizing buffer into the desired buffer conditions (for k_- determinations). Viscosities and osmotic pressures of sucrose and methylcellulose solutions were obtained from published values (Anderson, 1970; Wolf, 1986) or from the manufacturer.

Phalloidin Binding Kinetics and Affinity. The association rate constant of phalloidin binding to actin (k_{+Ph}) was determined at 22 °C from the dependence of k_{obs} on the phalloidin concentration (0.23−2.28 μM) at constant rhodamine phalloidin (1.8 μM) and actin filament (0.45 μM) concentrations. In the case of phalloidin and rhodamine phalloidin competing for a limited number of sites on an actin filament,

$$k_{obs} = k_{+Ph}[Ph] + k_{+RhPh}[RhPh] \qquad (5)$$

Therefore, k_{+Ph} is obtained from the slope of the line generated from plotting k_{obs} versus phalloidin concentration. The intercept yields $k_{+RhPh}[RhPh]$. The dissociation rate constants of both phalloidin derivatives are slow enough that they will not contribute significantly to k_{obs} and can be ignored.

The dissociation rate constant of phalloidin (k_{-Ph}) was determined from the rate of fluorescence enhancement when 7.2 μM rhodamine phalloidin was added to a sample of 1.0 μM actin filaments equilibrated with 1 molar equiv of phalloidin in 1X polymerizing buffer at 22 °C. The rate-limiting step under these conditions is the dissociation of bound phalloidin. Therefore, the rate of fluorescence enhancement arising from rhodamine phalloidin binding gives the dissociation rate constant of the initially bound phalloidin.

The affinity of phalloidin for actin was estimated from the ratio of the rate constants and from the reduction in equilibrium fluorescence of rhodamine phalloidin and actin over a range of phalloidin concentrations using the relation

$$K_{Ph} = \frac{1 + K_{RhPh}[RhPh]}{[Ph]_{0.5}} \qquad (6)$$

where K_{Ph} and K_{RhPh} are the association equilibrium constants for phalloidin and rhodamine phalloidin, respectively, [RhPh] is the rhodamine phalloidin concentration, and $[Ph]_{0.5}$ is the concentration of phalloidin which results in a 50% displacement of the initially bound rhodamine phalloidin (Huang *et al.*, 1992).

Nucleotide Exchange Kinetics. The dissociation rate constant of Mg^{2+}−ATP from actin (k_{-MgATP}) was measured from the fluorescence increase when 0.8−1.9 μM Mg^{2+}−ATP−actin was added to 200 μM ϵATP in 20 mM Tris (pH 8.0) and 1 mM $MgCl_2$ buffer at 22 °C (De La Cruz & Pollard, 1995). Free ATP was removed from ATP−actin with Dowex 1. The dissociation rate constant of ATP from Ca^{2+}−ATP−actin (k_{-CaATP}) was determined under similar conditions except $MgCl_2$ was replaced with 0.2 mM $CaCl_2$. The time course of fluorescence increase due to ϵATP binding was fitted with a nonlinear curve-fitting program. Frieden and Patane (1988) observed a greater k_{-ATP} as the ATP concentration was increased. We did not observe a dependence of k_{-MgATP} on the free ϵATP concentration under our experimental conditions of high divalent cation concentration and pH (data not shown).
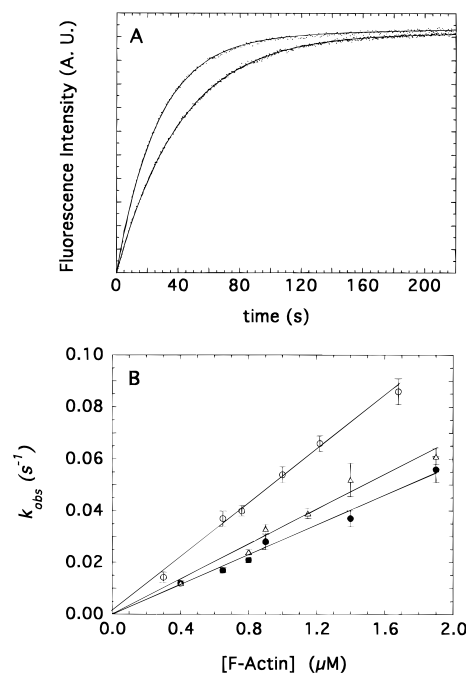

FIGURE 1: Kinetics of rhodamine phalloidin binding to actin filaments. (A) Time course of the change in fluorescence intensity after mixing 10 nM rhodamine phalloidin with 0.8 μM *S. cerevisiae* (left) or *Acanthamoeba* (right) actin filaments in 1X polymerizing buffer. The solid lines are the best fits to single exponentials. (B) Dependence of the observed rate constant (k_{obs}) for the association of rhodamine phalloidin and actin on the actin filament concentration: *S. cerevisiae* actin (○), *Acanthamoeba* actin (△), and rabbit skeletal muscle actin (●). The association rate constants (k_+) for rhodamine phalloidin binding are 5.1 (±0.2) × 10^4 M^{-1} s^{-1} for *S. cerevisiae* actin, 3.4 (±0.3) × 10^4 M^{-1} s^{-1} for *Acanthamoeba* actin, and 2.9 (±0.2) × 10^4 M^{-1} s^{-1} for rabbit skeletal muscle actin at 22 °C. Vertical bars are the standard deviation from the mean (n = 4−8 for yeast; n = 4−5 for *Acanthamoeba*; n = 4−8 for rabbit skeletal muscle actin from two different preparations of each).

RESULTS

(a) Rate Constant for Rhodamine Phalloidin Association with Actin Filaments. The time course of the fluorescence enhancement after mixing rhodamine phalloidin with *S. cerevisiae* actin filaments fits a single exponential (Figure 1A), like *Acanthamoeba* (Figure 1A) and rabbit skeletal muscle actin (not shown). The observed rate constants, k_{obs}, depend linearly on the concentrations of actin filaments for all three actins (Figure 1B). The slopes of the lines yield association rate constants for rhodamine phalloidin binding (k_{+RhPh}) of 5.1 (±0.2) × 10^4 M^{-1} s^{-1} for *S. cerevisiae* actin filaments and 3.4 (±0.3) × 10^4 M^{-1} s^{-1} for *Acanthamoeba* actin filaments at 22 °C. The k_{+RhPh} for rabbit skeletal muscle actin, 2.9 (±0.2) × 10^4 M^{-1} s^{-1}, confirms previous determinations of 2.8 × 10^4 M^{-1} s^{-1} (De La Cruz & Pollard, 1994) and 3 × 10^4 M^{-1} s^{-1} (Allen & Janmey, 1994). Partial saturation of filaments with one phalloidin per four actin subunits is reported (Orlova *et al.*, 1995) to alter the conformation of the filaments, but this has no effect on the association rate constant for rhodamine phalloidin and rabbit actin filaments (data not shown).

(b) Rate Constant for Rhodamine Phalloidin Dissociation from Actin Filaments. The dissociation rate constant of rhodamine phalloidin (k_{-RhPh}) was obtained by adding excess phalloidin to a sample of actin filaments equilibrated with rhodamine phalloidin (Figure 2). At 22 °C, rhodamine phalloidin dissociates with a rate constant of 0.0016 (±0.0002)
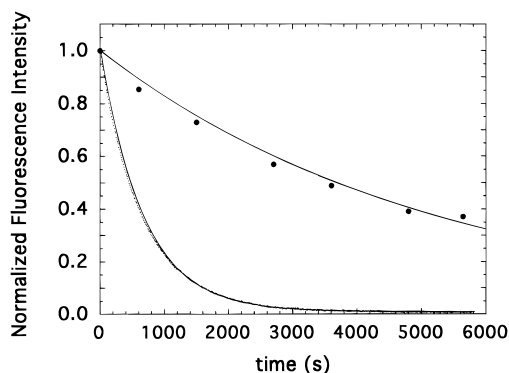
FIGURE 2: Time course of rhodamine phalloidin dissociation from actin filaments. Rhodamine phalloidin (10 nM) was equilibrated with 1.25 μM *S. cerevisiae* (left) or 1.9 μM *Acanthamoeba* (right) actin filaments for 2 h in 1X polymerizing buffer at 22 °C, and the fluorescence intensity was monitored upon addition of 40 μM phalloidin. Only the first 6000 s of the *Acanthamoeba* time course is shown. The solid lines are the best fits to single exponentials. The dissociation rate constants are 1.6 ($\pm$0.2) $\times$ 10^{-3} s^{-1} ($n = 5$) for *S. cerevisiae* actin, 1.7 ($\pm$0.2) $\times$ 10^{-4} s^{-1} ($n = 3$) for *Acanthamoeba* actin, and 2.6 $\times$ 10^{-4} s^{-1} ($n = 2$) for rabbit skeletal muscle actin (not shown).

s^{-1} ($n = 5$) from *S. cerevisiae* actin filaments and at 0.00017 ($\pm$0.00002) s^{-1} ($n = 3$) from *Acanthamoeba* actin filaments. The dissociation rate constant from rabbit skeletal muscle actin filaments, 0.00026 s^{-1} ($n = 2$), agreed with published values (Allen & Janmey, 1994; De La Cruz & Pollard, 1994). From the ratio of the rate constants, we calculate dissociation equilibrium constants (K_d) of 32 ($\pm$4) nM for *S. cerevisiae* actin, 5 ($\pm$1) nM for *Acanthamoeba* actin, and 9 ($\pm$2) nM for rabbit skeletal muscle actin.

(c) Thermodynamics of Rhodamine Phalloidin Binding. Eyring plots of the dependence of k_+ on the temperature for *Acanthamoeba* and rabbit skeletal muscle actin are linear over the temperature range examined and have identical slopes (Figure 3A), yielding activation enthalpies ($\Delta H^{\ddagger}$) of $\sim$2.3 kcal mol^{-1} (Table 1). The Eyring plot for *S. cerevisiae* actin is linear over a wide range of temperatures but changes slope at $\sim$12 °C (Figure 3A). At temperatures of >12 °C, the activation enthalpy ($\Delta H^{\ddagger}$) is 3.4 $\pm$ 0.1 kcal mol^{-1}.

Eyring plots of temperature dependence of k_- for all three actins are linear over the range examined (Figure 3B). The activation enthalpies ($\Delta H^{\ddagger}$) for dissociation of rhodamine phalloidin are 4.9 $\pm$ 0.4 kcal mol^{-1} for *S. cerevisiae* actin filaments, 3.9 $\pm$ 0.2 kcal mol^{-1} for *Acanthamoeba* actin filaments, and 4.5 $\pm$ 0.3 kcal mol^{-1} for rabbit skeletal muscle actin filaments.

By calorimetry, the ΔH° associated with rhodamine phalloidin binding to rabbit actin is -2.9 kcal mol^{-1} (Table 1). This value agrees closely with the ΔH° estimated from the difference in association and dissociation activation enthalpies (see Table 1 footnotes), consistent with a simple bimolecular mechanism for rhodamine phalloidin binding (De La Cruz & Pollard, 1994; Allen & Janmey, 1994). Table 1 summarizes all the kinetic and thermodynamic parameters for the binding of rhodamine phalloidin and actin filaments.

(d) Effects of pH, Ionic Strength, Viscosity, Filament Length, and Solvent Isotope on the Binding of Rhodamine Phalloidin and Muscle Actin. The association rate constant for rhodamine phalloidin binding to rabbit actin filaments is independent of pH over the range of pH 5.90$-$8.34 (data
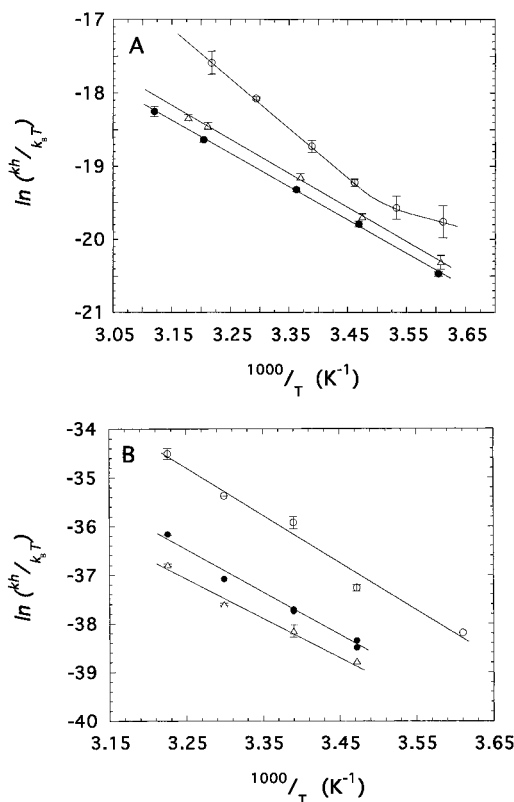

FIGURE 3: Temperature dependence of phalloidin binding kinetics. (A) Temperature dependence of the association rate constant of rhodamine phalloidin and actin filaments in 1X polymerizing buffer. The activation enthalpies ($\Delta H^{\ddagger}$) obtained from the slopes of the lines are 3.4 ($\pm$0.10) kcal mol^{-1} for *S. cerevisiae* actin (O) at temperatures of >12 °C, 2.3 ($\pm$0.05) kcal mol^{-1} for *Acanthamoeba* actin ($\triangle$), and 2.3 ($\pm$0.04) kcal mol^{-1} for rabbit skeletal muscle actin ($\bullet$). Vertical bars represent standard deviation from the mean ($n = 3-6$ for yeast; $n = 5-8$ for *Acanthamoeba*; $n = 5-6$ for rabbit skeletal muscle). (B) Temperature dependence of the dissociation rate constant of rhodamine phalloidin from actin filaments in 1X polymerizing buffer. The fluorescence intensity was monitored upon addition of 40 μM phalloidin to an equilibrated sample of 20 nM rhodamine phalloidin and actin filaments at the indicated temperatures. The activation enthalpies ($\Delta H^{\ddagger}$) for dissociation of rhodamine phalloidin are 4.9 ($\pm$0.4) kcal mol^{-1} for *S. cerevisiae* actin (O), 3.9 ($\pm$0.2) kcal mol^{-1} for *Acanthamoeba* actin ($\triangle$), and 4.5 ($\pm$0.3) kcal mol^{-1} for rabbit skeletal muscle actin ($\bullet$). Vertical bars represent the standard deviation from the mean ($n = 3-5$ for yeast; $n = 3$ for *Acanthamoeba*; $n = 3$ for rabbit skeletal muscle actin from two different preparations of each).

not shown) and ionic strength over the range of 50$-$500 mM KCl in the presence of 1 mM MgCl$_2$ (data not shown). Similarly, the dissociation rate constant for rhodamine phalloidin is unaffected by the absence of KCl or both KCl and MgCl$_2$ in 1X polymerizing buffer (data not shown). Shortening the length of the filaments with Cap Z (one per 233 actin subunits), the skeletal muscle capping protein (donated by Dr. J. F. Casella), does not affect the association rate (data not shown). Raising the solvent macroviscosity with methylcellulose (1$-$177 cp) has no significant effect on the association kinetics of rhodamine phalloidin and actin (data not shown). However, increasing the microviscosity with sucrose slows both association and dissociation of rhodamine phalloidin (panels A and B of Figure 4) with no net effect on the equilibrium binding affinity (Figure 4C). The association rate constant is not significantly different in water and 65% D$_2$O (data not shown).

Table 1: Thermodynamic and Kinetic Parameters for Rhodamine Phalloidin Binding to Actin Filaments at 22 °C

parameter[a]	rabbit skeletal muscle	*Acanthamoeba*	*S. cerevisiae*
k_+ (M^{-1} s^{-1})	2.9 ($\pm$0.2) $\times$ 10^4	3.4 ($\pm$0.3) $\times$ 10^4	5.1 ($\pm$0.2) $\times$ 10^4
k_- (s^{-1})	0.00026	0.00017 $\pm$ 0.00002	0.0016 $\pm$ 0.0002
K_d (nM)	9 $\pm$ 2	5 $\pm$ 1	32 $\pm$ 4
$\Delta H_a^{\ddagger}$ (kcal mol^{-1})	2.29 $\pm$ 0.04[b]	2.33 $\pm$ 0.05	3.40 $\pm$ 0.10
$\Delta G_a^{\ddagger}$ (kcal mol^{-1})	11.2 $\pm$ 0.02	11.2 $\pm$ 0.03	11.0 $\pm$ 0.05
$\Delta S_a^{\ddagger}$ (cal mol^{-1} K^{-1})	$-$30.2 $\pm$ 0.2	$-$30.2 $\pm$ 0.2	$-$25.8 $\pm$ 0.4
$T\Delta S_a^{\ddagger}$ (kcal mol^{-1})	$-$8.9 $\pm$ 0.1	$-$8.9 $\pm$ 0.1	$-$7.6 $\pm$ 0.1
$\Delta H_d^{\ddagger}$ (kcal mol^{-1})	4.5 $\pm$ 0.3	3.9 $\pm$ 0.2	4.9 $\pm$ 0.4
$\Delta G_d^{\ddagger}$ (kcal mol^{-1})	22.1	22.4 $\pm$ 0.1	21.1 $\pm$ 0.1
$\Delta S_d^{\ddagger}$ (cal mol^{-1} K^{-1})	$-$59.7	$-$62.7 $\pm$ 0.8	$-$54.9 $\pm$ 1.4
$T\Delta S_d^{\ddagger}$ (kcal mol^{-1})	$-$17.6	$-$18.5 $\pm$ 0.2	$-$16.2 $\pm$ 0.4
$\Delta H°$ (kcal mol^{-1})[c]	$-$2.2 $\pm$ 0.3	$-$1.6 $\pm$ 0.2	$-$1.5 $\pm$ 0.4
$\Delta G°$ (kcal mol^{-1})[d]	$-$10.9	$-$11.2 $\pm$ 0.1	$-$10.1 $\pm$ 0.1
$\Delta S°$ (cal mol^{-1} K^{-1})[e]	29.5	32.5 $\pm$ 0.8	29.1 $\pm$ 1.5
$T\Delta S°$ (kcal mol^{-1})	8.7	9.6 $\pm$ 0.2	8.6 $\pm$ 0.4
$\Delta H°$ (kcal mol^{-1})[f]	$-$2.9	ND[g]	ND

[a] The subscripts a and d refer to the association and dissociation reactions, respectively. [b] $n = 3-5$ where standard errors are indicated. [c] Calculated from $\Delta H° = \Delta H_a^{\ddagger} - \Delta H_d^{\ddagger}$. [d] Calculated from $\Delta G° = \Delta G_a^{\ddagger} - \Delta G_d^{\ddagger} = RT \ln K_d$. [e] Calculated from $\Delta S° = \Delta S_a^{\ddagger} - \Delta S_d^{\ddagger}$. [f] Calorimetric determination. [g] ND = not determined.

(e) Phalloidin Binding Kinetics and Affinity. The time course of the fluorescence enhancement after mixing a solution of rhodamine phalloidin and various concentrations of phalloidin with muscle actin filaments fits a single exponential as in Figure 1A (data not shown). The k_{obs} depends linearly on the concentration of phalloidin (Figure 5A). The slope of the line yields an association rate constant (k_{+Ph}) of 1.7 ($\pm$0.2) $\times$ 10^5 M^{-1} s^{-1} for phalloidin binding to muscle actin filaments at 22 °C. The k_{+RhPh} determined from the y-intercept divided by the concentration of rhodamine phalloidin is 2.6 ($\pm$0.7) $\times$ 10^4 M^{-1} s^{-1}, in agreement with previous determinations (Figure 1; De La Cruz & Pollard, 1994; Allen & Janmey, 1994).

The dissociation rate constant of unlabeled phalloidin (k_{-Ph}) was obtained by adding excess rhodamine phalloidin to a sample of actin filaments equilibrated with equimolar phalloidin (Figure 5B). Phalloidin dissociates with a rate constant of 0.00037 ($\pm$0.00003) s^{-1} ($n = 4$) from rabbit muscle actin filaments at 22 °C.

From the ratio of the rate constants, we calculate a dissociation equilibrium constant (K_d) of 2.1 ($\pm$0.3) nM for muscle actin and phalloidin at 22 °C. From the reduction in equilibrium fluorescence (the amplitudes of the transients) of rhodamine phalloidin (Figure 5C), we calculate a K_d of 0.5 ($\pm$0.2) nM using eq 6. This figure is less reliable than the ratio of the k's.

The temperature dependence of phalloidin binding was not investigated, but calorimetry shows that phalloidin binds actin filaments with a $\Delta H°$ of $-$13.6 ($\pm$0.7) kcal mol^{-1} ($n = 5$) at pH 7.0. Calorimetric titration with phalloidin shows a strict linear relationship between heat released ($\Delta H°$) and bound phalloidin until all sites on the filament are occupied. Therefore, the large negative $\Delta H°$ does not arise from the conformational change that occurs after phalloidin binds. The calorimetric $\Delta H°$ is independent of buffer ionization enthalpies, demonstrating that protons are neither released nor bound when phalloidin binds to actin.

(f) Nucleotide Exchange. The dissociation rate constants of Mg^{2+}-ATP (k_{-MgATP}) and Ca^{2+}-ATP (k_{-CaATP}) were measured by displacing bound ATP from Mg^{2+}-actin or Ca^{2+}-actin monomers with a large molar excess of ϵATP in 1 mM MgCl$_2$ or 0.2 mM CaCl$_2$, respectively (data not

shown). As previously reported by several labs [summarized in De La Cruz and Pollard (1995)], k_{-MgATP} is greater than k_{-CaATP} for rabbit skeletal muscle actin (Table 2). The rates of Mg^{2+}-ATP and Ca^{2+}-ATP dissociation from *Acanthamoeba* actin were similar to those of rabbit skeletal muscle actin under the experimental conditions examined (Table 2).

In contrast, k_{-MgATP} and k_{-CaATP} of *S. cerevisiae* actin are the same ($\sim$0.01 s^{-1}) at pH 8.0 and 22 °C (Table 2). Our value for the k_{-CaATP} of *S. cerevisiae* actin differs by less than a factor of 2 from that of Chen *et al.* (1993) obtained by a different method under slightly different buffer conditions. Miller *et al.* (1995) reported that ϵATP dissociates more rapidly from yeast actin than rabbit actin but did not examine the divalent cation specificity.

DISCUSSION

(a) Biochemical Differences among Actin Isoforms. The Lorenz *et al.* (1993) model of F-actin shows phalloidin interacting with neighboring subunits through both hydrogen bonds and hydrophobic interactions. Most of these amino acid residues are identical in all three actin types that we examined (Ng & Abelson, 1980; Gallwitz & Seidel, 1980; Vandekerckhove *et al.*, 1984), including R177 and R179 which are required for binding (Drubin *et al.*, 1993). The one exception is residue 201, which is valine in muscle, serine in *S. cerevisiae*, and threonine in *Acanthamoeba*. Thus, within the area of direct contact with phalloidin, substituting threonine for valine has little effect on the affinity while substitution with serine (*S. cerevisiae*) destabilizes the complex significantly.

If we consider the actin-phalloidin interface similar to the intramolecular interactions of a globular protein such as staphylococcal nuclease, the effects of these amino acid substitutions can be rationalized. Single substitution mutations in staphylococcal nuclease demonstrate that substitution of threonine for valine has little or no effect on the stable, native state, while serine substitutions tend to disrupt intramolecular interactions considerably, resulting in a less stable structure (Byrne *et al.*, 1995).

Amino acid substitutions far from the binding site may influence the flexibility of the actin filament and the binding
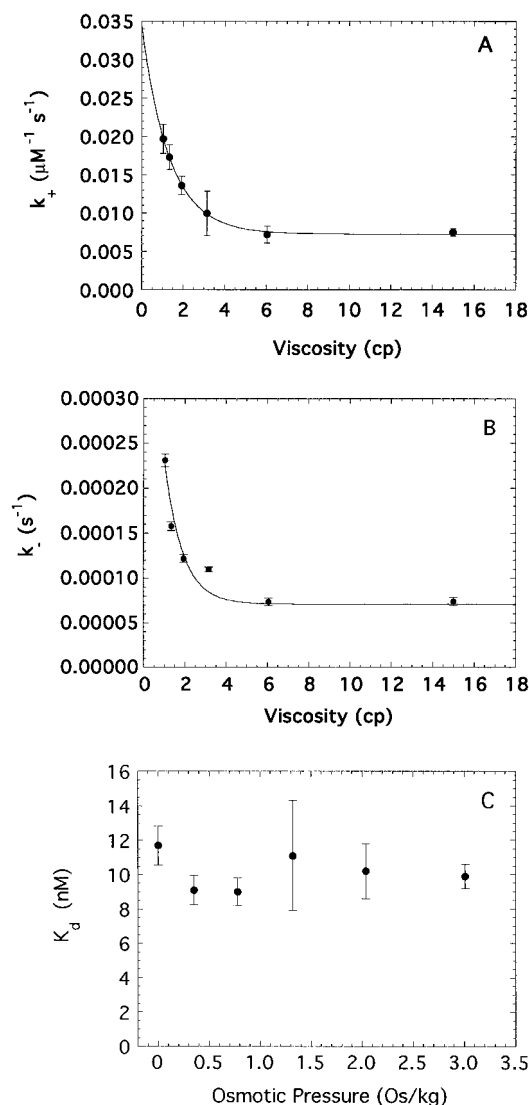
FIGURE 4: Effects of sucrose on rhodamine phalloidin binding kinetics and affinity. (A) Viscosity dependence of the association rate constant for rhodamine phalloidin binding to rabbit actin filaments in 1X polymerizing buffer. Vertical bars are standard deviations from the mean ($n = 4$). (B) viscosity dependence of rhodamine phalloidin dissociation from rabbit actin filaments in 1X polymerizing buffer. (C) Osmotic pressure dependence of rhodamine phalloidin equilibrium binding affinity calculated from the ratio of the rate constants. The sucrose concentrations are 0, 10, 20, 30, 40, and 50% (w/v) from left to right in all three panels.
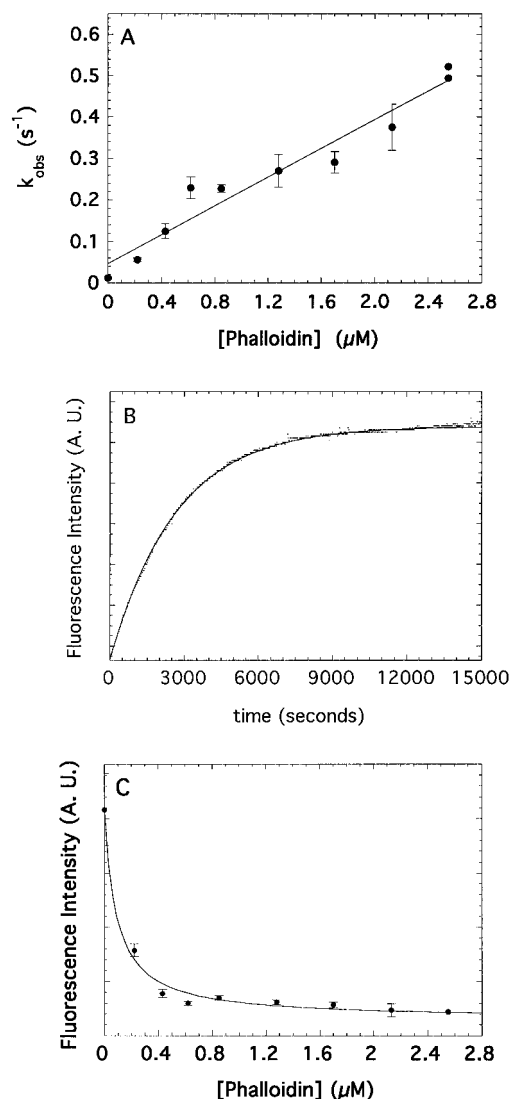

FIGURE 5: Kinetics and affinity of phalloidin binding to rabbit muscle actin filaments. (A) Phalloidin concentration dependence of the observed rate constant (k_{obs}) for the association of rhodamine phalloidin and actin in 1X polymerizing buffer at 22 °C. The slope of the line yields an association rate constant for phalloidin binding (k_{+Ph}) of 1.7 (± 0.2) $\times 10^5$ M^{-1} s^{-1}. The association rate constant for rhodamine phalloidin binding (k_{+RhPh}) estimated from the y-intercept of the line is 2.6 (± 0.7) $\times 10^4$ M^{-1} s^{-1}. Vertical bars are the standard deviation from the mean ($n = 4$). (B) Time course of phalloidin dissociation from actin filaments. Phalloidin (1.0 μM) was equilibrated with 1.0 μM actin filaments for 2 h in 1X polymerizing buffer at 22 °C, and the fluorescence intensity was monitored upon addition of 7.2 μM rhodamine phalloidin. The solid line is the best fit to a single exponential, yielding a dissociation rate constant of phalloidin (k_{-Ph}) of 3.7 (± 0.3) $\times 10^{-4}$ s^{-1} ($n = 4$). (C) Dependence of the equilibrium fluorescence of actin and rhodamine phalloidin on the concentration of competing phalloidin. The curve represents the best fit to eq 6. The dissociation equilibrium constant determined from this analysis is 0.5 (± 0.2) nM. The ratio of the rate constants gives a more accurate estimate of the dissociation equilibrium constant of 2.1 (± 0.3) nM.

kinetics of phalloidin. The rigidity of the polymer depends on the number of interactions between the subunits (Tirion *et al.*, 1995). *S. cerevisiae* differs from both muscle and *Acanthamoeba* at several positions thought to participate in intermolecular bonds in the filament: nine residues (V43I, L110M, E167A, Y169F, A170S, F266V, M269L, I289V, and T324S) in the model of Holmes *et al.* (1990) and six (E167A, Y169F, A170S, Q263H, F266V, and M269L) in the refined F-actin model of Tirion *et al.* (1995). *S. cerevisiae* actin filaments appear qualitatively less rigid (Kron *et al.*, 1992) and fragment more easily (Buzan & Frieden, 1996) than rabbit skeletal muscle actin filaments, so these substitutions may allow *S. cerevisiae* actin filaments to breathe more easily than rabbit skeletal muscle and *Acanthamoeba* actin filaments, allowing phalloidin to associate (Figure 1) and dissociate (Figure 2) more readily.

Labeling the *S. cerevisiae* actin cytoskeleton requires higher concentrations of phallotoxin than staining of animal

or protozoan cells (Szczesna & Lehrer, 1993; Wong *et al.*, 1983; Amatruda & Cooper, 1992). The lower affinity of rhodamine phalloidin for yeast actin (Table 1) explains these observations. Novel yeast actin-binding proteins may also interfere with binding of rhodamine phalloidin. Two precedents in animal cells are gelsolin (Allen & Janmey, 1994) and nebulin (Ao & Lehrer, 1995).

Our values for the rate constants for ATP dissociation (Table 2) explain why the affinity of *S. cerevisiae* actin for

Table 2: Dissociation Rate Constants of ATP from Actin Monomers[a]

[divalent cation]	rabbit skeletal muscle	*Acanthamoeba*	*S. cerevisiae*
0.2 mM $CaCl_2$	0.0016 ± 0.0006 s^{-1}	0.0020 ± 0.0017 s^{-1}	0.010 ± 0.002 s^{-1}
1 mM $MgCl_2$	0.008 ± 0.003 s^{-1}	0.010 ± 0.001 s^{-1}	0.009 ± 0.003 s^{-1}

[a] $n = 3-5$.

$Ca^{2+}-ATP$ is ~3-fold weaker than that of rabbit skeletal muscle actin and the same as the affinities of both actins for $Mg^{2+}-ATP$ (Chen *et al.*, 1995). The dissociation rate constants of the metal−nucleotide complexes determine the different binding affinities and not the association rate constants (De La Cruz & Pollard, 1995).

The amino acids in contact with ATP are the same in all three actins, so the greater k_{-CaATP} of *S. cerevisiae* actin must result from changes outside the nucleotide binding region. Residues 137−144 form an α-helix suggested to provide a hinge for subdomain motions (Tirion & ben-Avraham, 1993; Holmes *et al.*, 1993). A substitution in this helix (Ala144 in rabbits and *Acanthamoeba*, Ser144 in *S. cerevisiae*) may contribute to the unique nucleotide exchange behavior of yeast actin.

(b) Energetics of Phalloidin Binding. A simple bimolecular association reaction can describe the binding of rhodamine phalloidin to actin filaments (De La Cruz & Pollard, 1994; Allen & Janmey, 1994):

$$\text{actin} + \text{RhRh} \underset{k_-}{\overset{k_+}{\rightleftharpoons}} \text{actin}-\text{RhRh}$$
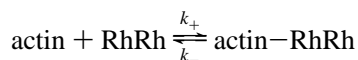
The temperature dependence of the rate constants (Figure 3A,B) indicates that there is a small enthalpic difference ($\Delta H^{\ddagger}$) between the reactants and the transition state for both the association and dissociation reactions (Table 1). At equilibrium, the net change in enthalpy between the free and bound states (ΔH°) is also very small (Table 1). Consequently, the free energies of rhodamine phalloidin binding ($\Delta G^{\ddagger}$ and ΔG°) are dominated by entropic changes ($\Delta S^{\ddagger}$ and ΔS°). It is difficult to assign precisely the factors that contribute to the entropy changes, which may include contributions from the solvent, phalloidin, and actin. However, given the extent of hydrophobic interactions in the proposed phalloidin binding site (Lorenz *et al.*, 1993), it seems likely that the positive ΔS° arises from changes in the solvent, perhaps due to disruption of ordered water molecules on actin and phalloidin. In addition, phalloidin increases the torsional flexibility of actin filaments (Prochniewicz *et al.*, 1996) which will also contribute to a positive ΔS°.

Actin binds phalloidin and rhodamine phalloidin differently. The association rate constant of phalloidin (Figure 5A) is greater than it is for rhodamine phalloidin (Figure 1). The dissociation rate constants of the two analogs are similar (Figures 2 and 5B). Consequently, the affinity of actin for phalloidin is about 5-fold greater than for rhodamine phalloidin (Huang *et al.*, 1992). The equilibrium binding affinity of ~2.1 nM yields a free energy ($\Delta G^{\ddagger}$) for phalloidin binding of about −11.7 kcal mol^{-1}. The ΔH° is more favorable for phalloidin binding than for rhodamine phalloidin (−13.6 kcal mol^{-1} for phalloidin versus −2.9 kcal mol^{-1} for rhodamine phalloidin at pH 7.0)! The big difference in the ΔH° may be due to specific bond formation that is precluded by the associated fluorophore.

Although substoichiometric phalloidin binding is reported to induce a long range change in the electron microscopic structure of actin filaments (Orlova *et al.*, 1995), this conformational change does not affect the ΔH° for phalloidin binding. By calorimetry, there is a strict linear dependence of the heat released (ΔH°) on bound phalloidin until all phalloidin binding sites on the filament are occupied. With a ΔH° of −13.6 kcal mol^{-1}, the ΔS° for phalloidin binding must be negative in contrast to the positive ΔS° of rhodamine phalloidin (Table 1). A negative ΔS° for phalloidin binding has been reported (Le Bihan & Gicquaud, 1991) and may result from interactions of phalloidin-labeled filaments with the solvent (Cuneo *et al.*, 1995).

(c) Why Is Rhodamine Phalloidin Binding to Actin Filaments So Slow? The association rate constant of rhodamine phalloidin binding to actin filaments (~10^4 M^{-1} s^{-1}) is extremely low for the bimolecular association of a peptide and macromolecule [see De La Cruz and Pollard (1994)]. The small association rate constant suggested a model where the phalloidin binding sites on an actin filament are not readily exposed but become accessible as the filament experiences thermal fluctuations in shape, or breathes (De La Cruz & Pollard, 1994). In this model, binding is limited by the accessibility of the sites.

We can eliminate other factors that decrease the association rates of other molecules, including electrostatic repulsion, slow protonation reactions, and slow rearrangement of water molecules (Ferscht, 1984; Bartlett & Marlowe, 1987). The association rate of rhodamine phalloidin is independent of the ionic strength (50−500 mM KCl) and pH (5.90−8.34), suggesting that neither is responsible for the slow binding kinetics. Since osmotic stress (Rand *et al.*, 1993; Parsegian *et al.*, 1995) does not affect the affinity of actin and rhodamine phalloidin (Figure 4C), and 65% D_2O does not generate a solvent isotope effect on the association reaction (data not shown), we can exclude hydration/dehydration as the rate-limiting step for binding. It is important to stress that this does not mean that rearrangement of water molecules does not occur when rhodamine phalloidin binds, simply that it does not limit the rate of the reactions.

We suggest that sucrose reduces the rates of rhodamine phalloidin binding and dissociation without a change in the binding affinity by suppressing actin filament dynamics. Suppressed breathing would inhibit both association and dissociation. The effect is not due to changes in the chemical potential of the reactants since sucrose does not change the binding affinity (Figure 4C). Sucrose must therefore dampen some kinetic process. Solvent microviscosity restricts the structural dynamics and conformational flexibility of proteins (Gavish & Werber, 1979; Somogyi *et al.*, 1988; Priev *et al.*, 1995) and limits the accessibility of phalloidin binding sites.

The association rate constant for phalloidin is ~6-fold greater than that for rhodamine phalloidin (Figure 5A), so the fluorophore slows binding significantly. The effect is less dramatic for dissociation (Figure 5B). The different

association rates are not a consequence of solvent interactions with the bulky hydrophobic fluorophore as explained above but may result from the different dimensions and/or conformational degrees of freedom (Lee *et al.*, 1994) lost upon binding of the two analogs. Although phalloidin binds actin filaments more rapidly than rhodamine phalloidin, its binding is still much slower than the binding of other proteins, suggesting that filament breathing limits the rate of phalloidin binding.

REFERENCES

Allen, P. G., & Janmey, P. A. (1994) *J. Biol. Chem. 269*, 32916–32923.

Amatruda, J. F., & Cooper, J. A. (1992) *J. Cell. Biol. 117*, 1067–1076.

Anderson, N. G. (1970) in *CRC Handbook of Biochemistry, Selected Data for Molecular Biology, 2nd Edition* (Sober, H. A., Ed.) pp J288–J291, CRC Press, Boca Raton, FL.

Ao, X., & Lehrer, S. S. (1995) *J. Cell Sci. 108*, 3397–3403.

Bartlett, P. A., & Marlow, C. K. (1987) *Biochemistry 26*, 8553–8561.

Blanchoin, L., Didry, D., Carlier, M.-F., & Pantaloni, D. (1996) *J. Biol. Chem. 271*, 12380–12386.

Buzan, J. M., & Frieden, C. (1996) *Proc. Natl. Acad. Sci. U.S.A. 93*, 91–95.

Byrne, M. P., Manuel, R. L., Lowe, L. G., & Stites, W. E. (1995) *Biochemistry 34*, 13949–13960.

Chen, X., Cook, R. K., & Rubenstein, P. A. (1993) *J. Cell. Biol. 123*, 1185–1195.

Chen, X., Peng, J., Pedram, M., Swenson, C. A., & Rubenstein, P. A. (1995) *J. Biol. Chem. 270*, 11415–11423.

Cook, R. K., & Rubenstein, P. A. (1992) in *The Cytoskeleton: A Practical Approach* (Carraway, K. L., & Carraway, C. A. C., Eds.) pp 99–122, Oxford University Press, New York.

Cuneo, P., Trombetta, G., Magri, E., & Grazi, E. (1995) *Biochem. Biophys. Res. Commun. 211*, 614–618.

De La Cruz, E. M., & Pollard, T. D. (1994) *Biochemistry 33*, 14387–14392.

De La Cruz, E. M., & Pollard, T. D. (1995) *Biochemistry 34*, 5452–5461.

Drubin, D. G., Jones, H. D., & Wertman, K. (1993) *Mol. Biol. Cell 4*, 1277–1294.

Estes, J. E., Selden, L. A., & Gershman, L. C. (1981) *Biochemistry 20*, 708–712.

Eyring, H. (1935) *Chem. Rev. 17*, 65–77.

Ferscht, A. (1984) *Enzyme structure and mechanism*, W. H. Freeman & Company, New York.

Frieden, C., & Patane, K. (1988) *Biochemistry 27*, 3812–3820.

Gallwitz, D., & Seidel, R. (1980) *Nucleic Acids Res. 8*, 1043–1059.

Gavish, B., & Werber, M. M. (1979) *Biochemistry 18*, 1269–1274.

Gershman, L. C., Selden, L. A., Kinosian, H. J., & Estes, J. E. (1994) in *Actin: Biophysics, Biochemistry, and Cell Biology*, pp 35–49, Plenum Press, New York.

Goldman, W. H., & Isenberg, G. (1993) *FEBS Lett. 336*, 408–410.

Holmes, K. C., Popp, D., Gebhard, W., & Kabsch, W. (1990) *Nature 347*, 44–49.

Holmes, K. C., Sander, C., & Valencia, A. (1993) *Trends Cell Biol. 3*, 53–59.

Houk, T. W., & Ue, K. (1974) *Anal. Biochem. 62*, 66–74.

Huang, Z., Haugland, R. P., You, W., & Haugland, R. P. (1992) *Anal. Biochem. 200*, 199–204.

Kabsch, W., Mannherz, H. G., Suck, D., Pai, E. F., & Holmes, K. C. (1990) *Nature 347*, 37–44.

Kinosian, H. J., Selden, L. A., Estes, J. E., & Gershman, L. C. (1992) *J. Biol. Chem. 268*, 8683–8691.

Kron, S. J., Drubin, D. G., Botstein, D., & Spudich, J. A. (1992) *Proc. Natl. Acad. Sci. U.S.A. 89*, 4466–4470.

Kuhlman, P. A., Ellis, J., Critchley, D. R., & Bagshaw, C. R. (1994) *FEBS Lett. 339*, 297–301.

Le Bihan, T., & Gicquaud, C. (1991) *Biochem. Biophys. Res. Commun. 181*, 542–547.

Lee, K. H., Xie, D., Freire, E., & Amzel, L. M. (1994) *Proteins: Struct., Funct., Genet. 20*, 68–84.

Lorenz, M., Popp, D., & Holmes, K. C. (1993) *J. Mol. Biol. 234*, 826–836.

MacLean-Fletcher, S., & Pollard, T. D. (1980) *Biochem. Biophys. Res. Commun. 96*, 18–27.

Miller, C. J., Cheung, P., White, P., & Reisler, E. (1995) *Biophys. J. 68*, 50s–54s.

Miyamoto, Y., Kuroda, M., Munekata, E., & Masaki, T. (1986) *J. Biochem. 100*, 1677–1680.

Ng, R., & Abelson, J. (1980) *Proc. Natl. Acad. Sci. U.S.A. 77*, 3912–3916.

Orlova, A., Prochniewicz, E., & Egelman, E. H. (1995) *J. Mol. Biol. 245*, 598–607.

Parsegian, V. A., Rand, R. P., & Rau, D. C. (1995) *Methods Enzymol. 259*, 43–94.

Pollard, T. D. (1984) *J. Cell Biol. 99*, 769–777.

Press, W. H., Flannery, B. P., Teukolsky, S. A., & Vetterling, W. T. (1987) in *Numerical Recipes*, pp 550–560, Cambridge University Press, Cambridge, U.K.

Priev, A., Almagor, A., Yedgar, S., & Gavish, B. (1996) *Biochemistry 35*, 2061–2066.

Prochniewicz, E., Zhang, Q., Howard, E. C., & Thomas, D. D. (1996) *J. Mol. Biol. 255*, 446–457.

Rand, R. P., Fuller, N. L., Butko, P., Francis, G., & Nicholls, P. (1993) *Biochemistry 32*, 5925–5929.

Somogyi, B., Norman, J. A., Zempel, L., & Rosenberg, A. (1988) *Biophys. Chem. 32*, 1–13.

Spudich, J. A., & Watt, S. (1971) *J. Biol. Chem. 246*, 4866–4871.

Szczesna, D., & Lehrer, S. S. (1993) *J. Muscle Res. Cell Motil. 14*, 594–597.

Tirion, M. M., & ben-Avraham, D. (1993) *J. Mol. Biol. 230*, 186–195.

Tirion, M. M., ben-Avraham, D., Lorenz, M., & Holmes, K. C. (1995) *Biophys. J. 68*, 5–12.

Vandekerckhove, J., Lal, A. A., & Korn, E. D. (1984) *J. Mol. Biol. 172*, 141–147.

Wieland, T., & Faulstich, H. (1978) *Crit. Rev. Biochem. 5*, 185–260.

Wolf, A. V., Brown, M. G., & Prentiss, P. C. (1986) in *CRC Handbook of Chemistry and Physics* (Weast, R. T., Ed.) pp D219, D262, CRC Press, Boca Raton, FL.

Wong, A. J., Pollard, T. D., & Herman, I. M. (1983) *Science 219*, 867–869.